



# Preparation and characterization of isatin complexed with Cu supported on 4-(aminomethyl) benzoic acid-functionalized Fe<sub>3</sub>O<sub>4</sub> nanoparticles as a novel magnetic catalyst for the Ullmann coupling reaction

Mohammad Mehdi Khodaei<sup>1</sup> · Abdolhamid Alizadeh<sup>1</sup> · Maryam Haghipoor<sup>1</sup>

Received: 12 October 2018 / Accepted: 28 January 2019  
© Springer Nature B.V. 2019

## Abstract

Isatin complexed with Cu supported on 4-(aminomethyl) benzoic acid-functionalized Fe<sub>3</sub>O<sub>4</sub> nanoparticles (Cu-IS-AMBA-MNPs) as a new catalyst was designed, prepared and characterized by appropriate analyses. The heterogeneous reusable catalyst was successfully used for the efficient and widespread syntheses of diaryl ethers and diarylamines via the Ullmann coupling reaction. This green catalyst was easily removed, reused several times with no significant loss of its activity, and provided a clean synthesis with excellent yield and reduced time.

**Keyword** Magnetically recoverable nanocatalyst · Ullman coupling reaction · Nanoparticles · Diaryl ethers · Copper

## Introduction

Diaryl ethers and diarylamines are a class of important organic compounds in many biologically active natural products and play significant roles in the chemical industry and in medicinal chemistry [1, 2]. A large number of them have displayed particular and significant biological and pharmacological activities such as the isodityrosine family and its derivatives (e.g., the antibiotic vancomycin and the antitumor bouvardin) and commercial dyes [3–6]. Diaryl ethers have received the interests of investigators during this decade [2].

Traditionally, aryl ethers are prepared with Ullmann-type reactions between phenols and aryl halides mediated with a transition metal such as Pd and Cu [7–10]. This procedure is mostly performed at high temperatures and needs stoichiometric amounts of copper [11]. The Ullmann reaction was reported for the

✉ Mohammad Mehdi Khodaei  
mmkhoda@razi.ac.ir

<sup>1</sup> Department of Organic Chemistry, Razi University, Kermanshah 67149-67346, Iran

first time in 1901 and has for a long time been applied by chemists and researchers to form a C–C bond between two aromatic nuclei in the presence of copper powder as a catalyst [12, 13]. Copper-based catalysts, because of their low-priced raw materials, simple working and low toxicity are more applicable and attractive than Pd-based catalysts to form the C–O bond in diaryl ethers [14].

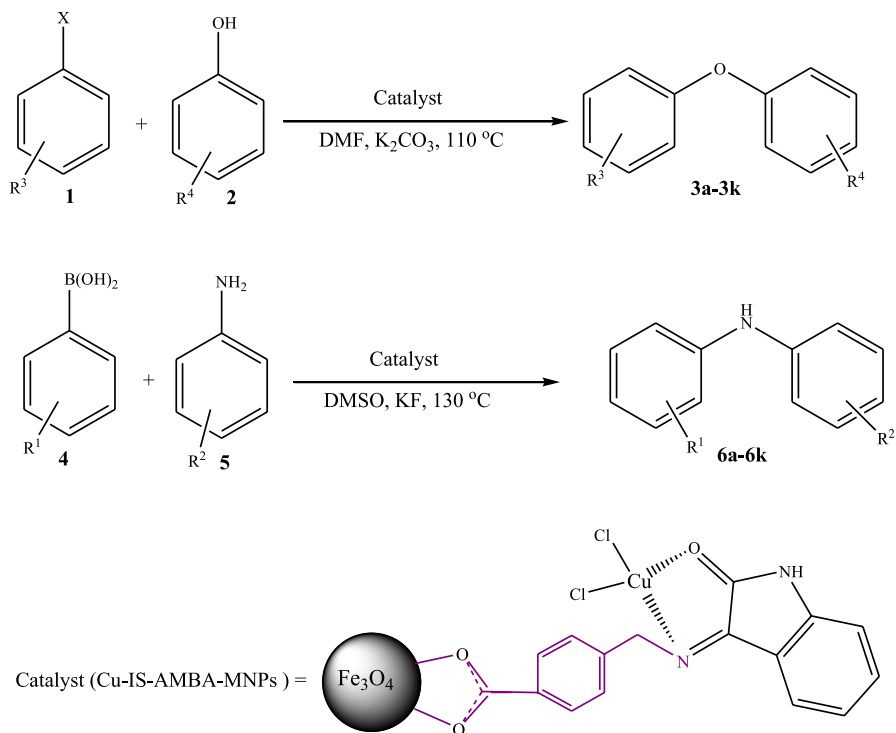
In recent decades, principal investigations have been handled and introduced in promoting the Cu-catalyzed Ullmann coupling reaction by using heterogeneous reusable catalysts [15–18] and many unique ligands. Some of them include 1,10-phenanthroline and its derivatives [19], ethylene glycol [20], diethylsali-cylamide, oxime-type and Schiff-base ligands [21], thiophene-2-carboxylate [22], bidentate phosphines [23], and diphosphinidene cyclobutane [24], 2,2,6,6-tetra-methylheptane-3,5-dione [25], phosphazene P4-tBu base [26], and *N,N*-dimethyl-glycine [27].

The importance of copper nanomaterial for organic chemistry reactions is undisputable. Copper nanoparticles have been used as a heterogeneous catalyst in various chemical transformations. Copper nanoparticle-catalyzed reactions are advantageous over conventional metal-catalyzed reactions in terms of better yields, shorter reaction times, low catalyst loading, high atom economy, inexpensiveness, and recyclability of the catalyst. It has been shown that most of the transformations proceed mechanistically via the formation of organometallic intermediates [C–Cu–X] during the interaction with copper nanoparticles [28].

In spite of considerable progress in the heterogeneous recoverable copper-catalyzed Ullmann reaction, the reusability of the catalyst support still attracts much attention. Carbon nanotubes (CNTs) have been widely studied as supports for depositing of metal nanoparticles as heterogeneous catalysts due to their unusual structure, excellent electronic conductivity, and enhanced approachability of reactants to the active sites [27, 29].

Also, magnetic nanoparticles (MNPs) can be used as supports in the preparation of heterogeneous recoverable catalysts for the Ullmann reaction. They have several unique magnetic properties including superparamagnetic, high coercivity, low Curie temperature, high magnetic susceptibility, and large surface-to-volume ratio. Development of suitable surface coating for efficient protection strategies to maintain the stability of MNPs is significant and necessary [30]. Surface functionalized MNPs have been extensively used in biotechnology and catalysis [31–35]. The design of new magnetically separable systems has attracted major consideration in recent decades as an appealing choice to enhance the efficient separation of heterogeneous nanocatalysts from products by their response to an external magnetic field [36, 37]. Eco-friendliness and biodegradability as well as excellent magnetic properties can be indicated for functional many organic compounds grafted to MNPs [38–41].

Here, we report a biocompatible catalyst for the Ullmann coupling reaction between aryl halides with phenols and aryl boronic acid with anilines using isatin complexed with Cu supported on 4-(aminomethyl) benzoic acid-functionalized Fe<sub>3</sub>O<sub>4</sub> nanoparticles (Cu-IS-AMBA-MNPs) as a novel heterogeneous recoverable nanocatalyst (Scheme 1). Isatin has been used as a Schiff base connected to Cu supported on AMBA-MNPs and characterized by different techniques, such as SEM, XRD, TGA, FT-IR, VSM, EDX and ICP-AES.



**Scheme 1** Ullmann coupling reaction with Cu-IS-AMBA-MNPs

## Experimental

### Chemicals and apparatus

The X-ray powder diffraction (XRD) of the prepared catalyst was performed on a Philips PW 1830 X-ray diffractometer with a  $\text{CuK}\alpha$  source ( $\lambda = 1.5418 \text{ \AA}$ ) in a range of Bragg's angle ( $10^\circ$ – $80^\circ$ ) at room temperature. Fourier-transform infrared (FT-IR) spectra were recorded using a FT-IR spectrometer (Vector 22, Bruker) in the range of  $400$ – $4000 \text{ cm}^{-1}$  at room temperature. Scanning electron microscopy (SEM) analysis was carried out using a VEGA//TESCAN KYKY-EM 3200 microscope (acceleration voltage  $26 \text{ kV}$ ). The spectrum of elemental analysis of the catalyst was recorded by energy dispersive X-ray (EDX; VEGA3 XUM/TESCAN). Thermogravimetric analysis (TGA) was carried out on a Stanton Red craft STA-780 (London, UK). NMR spectra were recorded with a Bruker DRX-400 ADVANCE instrument ( $300.1 \text{ MHz}$  for  $^1\text{H}$ ,  $75.4 \text{ MHz}$  for  $^{13}\text{C}$ ). The spectra were measured in  $\text{DMSO-}d_6$  as a solvent. Magnetic measurements were performed using a vibration sample magnetometer (VSM, MDK, and Model 7400) analysis. The metal loading was detected by an inductively coupled plasma-atomic emission spectrometer (ICP-AES). Melting points were measured on an Electrothermal 9100 apparatus.

## General procedure

### Preparation of 4-(aminomethyl) benzoic acid functionalized MNPs (AMBA-MNPs)

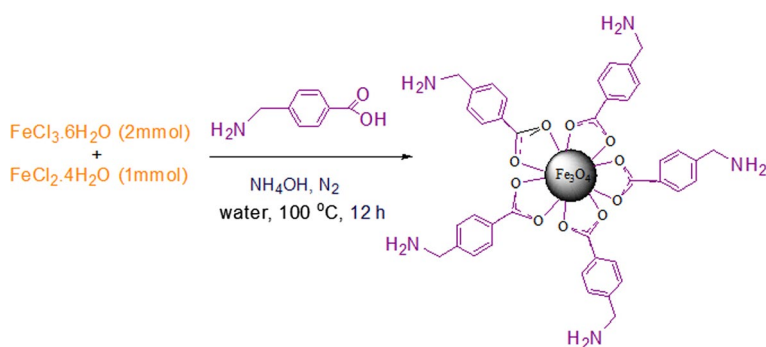
First, the MNPs were synthesized using the coprecipitation method described in the literature [42]. In a typical procedure,  $\text{FeCl}_3 \cdot 6\text{H}_2\text{O}$  (2.43 g, 0.09 mol) and  $\text{FeCl}_2 \cdot 4\text{H}_2\text{O}$  (0.89 g, 0.0045 mol) were dissolved in 100 mL of deionized water and the solution was sonicated until the salts completely dissolved. Then, 0.3 g of AMBA in 10 mL of  $\text{NH}_4\text{OH}$  solution was added to the prepared mixture with vigorous stirring under constant nitrogen flow to form a black suspension which was refluxed at 100 °C for 12 h. Then, AMBA-MNPs nanoparticles were separated from the aqueous solution by a magnetic field, washed with deionized water five times and subsequently dried in an oven overnight (Scheme 2).

### Preparation of supported isatin on AMBA-MNP<sub>5</sub> nanoparticles (IS-AMBA-MNPs)

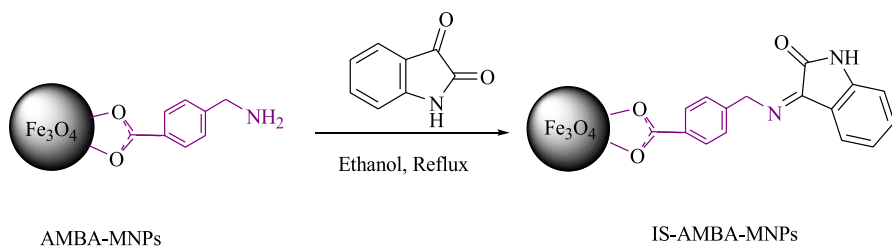
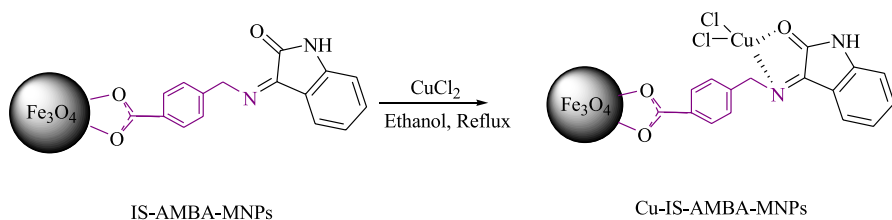
The prepared AMBA-MNPs (1 g) were scattered in 50 mL of ethanol using sonication for 30 min, and then 0.2 g of isatin (IS) was added to the mixture to form the black suspension. Next, this suspension was refluxed with strong stirring for 6 h. The IS-AMBA-MNPs were separated from the aqueous solution by magnetic decantation, washed with deionized water several times and dried in an oven overnight (Scheme 3). All of the synthesis steps were carried out under  $\text{N}_2$  flow.

### Preparation of copper supported on IS-AMBA-MNPs (Cu-IS-AMBA-MNPs)

The obtained IS-AMBA-MNPs (0.5 g) were dispersed in 50 mL of ethanol by sonication for 30 min, and then 0.045 g of  $\text{CuCl}_2$  added to the above mixture. A brown suspension was formed and refluxed with vigorous stirring for 8 h. The catalyst (Cu-IS-AMBA-MNPs) was separated from the solution by an external magnet, washed with deionized water several times, and dried in an oven overnight (Scheme 4). The whole synthesis was carried out under  $\text{N}_2$  flow.



**Scheme 2** Preparation of AMBA-MNPs

**Scheme 3** Preparation of IS-AMBA-MNPs**Scheme 4** Preparation of Cu-IS-AMBA-MNPs

### General procedure for the synthesis of diaryl ethers and diarylamines via Ullmann coupling reaction using Cu-IS-AMBA-MNPs as the catalyst

#### General procedure for *O*-arylation reactions

To prepare diaryl ethers using the Ullmann coupling reaction via *O*-arylation reactions, aryl halide (1 mmol), phenol derivative (1 mmol) and 0.2 g (1.5 mmol) of  $K_2CO_3$  in DMF (5 mL) were placed into a round-bottom flask containing 0.05 g (0.02 mmol) of the catalyst. The above mixture was refluxed at 110 °C for 3 h under vigorous stirring. When the reaction was complete, the reaction mixture was cooled and the solvent was removed under reduced pressure. Then, the mixture was diluted with  $CH_2Cl_2$  and the catalyst was separated by an external magnet. The filtrate was evaporated on a rotary evaporator and the crude product was purified by column chromatography using ethyl acetate/*n*-hexane.

#### General procedure for *N*-arylation reactions

The mixture of phenylboronic acid (1 mmol), aromatic amine (1.2 mmol) and 0.12 g (2 mmol) of KF in DMSO (4 mL) were added to Cu-IS-AMBA-MNPs (0.06 g, 0.025 mmol) at 130 °C under nitrogen atmosphere for 2 h with vigorous stirring. Then, after completion of the reaction, the catalyst was separated by an external magnet and washed with dry  $CH_2Cl_2$  three times and checked for its reusability. The solvent of the reaction mixture was evaporated by a rotary evaporator and then ethyl acetate and water were added to the residue. The organic layer was dried over anhydrous  $MgSO_4$ . The solvent was evaporated under

reduced pressure and the crude product was purified by column chromatography using ethyl acetate/*n*-hexane.

### Selected spectra for a few products are given below

4-Nitrophenyl 3-methylphenyl ether (Table 2, entry 5): m.p.: 62–63 °C; IR (KBr):  $\nu_{\max}$  = 3120, 2925, 2857, 1567, 1348, 1094  $\text{cm}^{-1}$ ;  $^1\text{H}$  NMR (400.13 MHz, DMSO):  $\delta$  = 2.32 (s, 3H,  $\text{CH}_3$ ), 7.28–7.38 (m, 3H), 7.42 (s, 1H), 7.53 (d, 2H,  $J$  = 8.8 Hz), 7.62 (d, 2H,  $J$  = 8.8 Hz) ppm.;  $^{13}\text{C}$  NMR (100.6 MHz, DMSO):  $\delta$  = 26.4, 123.1, 124.7, 126.0, 126.1, 127.2, 127.3, 128.1, 128.7, 129.3, 133.1 ppm.

2-Phenoxynaphthalene (Table 2, entry 6): m.p.: 97–98 °C; IR (KBr):  $\nu_{\max}$  = 3067, 2920, 1567, 1349, 1097  $\text{cm}^{-1}$ ;  $^1\text{H}$  NMR (400.13 MHz, DMSO):  $\delta$  = 7.33–7.75 (m, 7H), 7.85 (d, 2H,  $J$  = 8.0 Hz), 8.28 (d, 2H,  $J$  = 8.0 Hz) ppm.;  $^{13}\text{C}$  NMR (100.6 MHz, DMSO):  $\delta$  = 119.2, 120.3, 121.3, 123.0, 124.8, 126.0, 126.1, 127.2, 127.3, 128.1, 128.6, 129.4, 132.8, 133.2 ppm.

3-Nitrophenyl-2,6-dimethoxyphenyl ether (Table 2, entry 12): m.p.: 35–37 °C;  $^1\text{H}$  NMR (400.13 MHz, DMSO):  $\delta$  = 4.10 (s, 6H,  $\text{OCH}_3$ ), 6.59–6.67 (m, 3H), 7.17–7.19 (m, 2H), 7.31–7.37 (m, 2H) ppm.;  $^{13}\text{C}$  NMR (100.6 MHz, DMSO):  $\delta$  = 52.0, 118.1, 118.6, 119.9, 120.3, 124.7, 127.3, 129.8, 131.1, 131.5, 133.6 ppm.; anal. calcd. for  $\text{C}_{14}\text{H}_{13}\text{NO}_5$  (275.08): C, 61.09; H, 4.76; N, 5.09%; found: C, 61.40; H, 4.79; N, 5.04%.

3-Nitrophenyl-2,6-dimethylphenyl ether (Table 2, entry 13): m.p.: 42–43 °C;  $^1\text{H}$  NMR (400.13 MHz, DMSO):  $\delta$  = 2.12 (s, 6H,  $\text{CH}_3$ ), 7.03–7.10 (m, 3H), 7.24–7.27 (m, 3H), 7.35 (s, 1H) ppm.;  $^{13}\text{C}$  NMR (100.6 MHz, DMSO):  $\delta$  = 20.3, 120.6, 120.9, 123.2, 126.5, 127.2, 128.1, 129.6, 130.0, 132.0, 135.0 ppm.; anal. calcd. for  $\text{C}_{14}\text{H}_{13}\text{NO}_3$  (243.09): C, 69.12; H, 5.39; N, 5.76%; found: C, 69.40; H, 5.43; N, 5.71%.

Diphenylamine (Table 4, entry 1): m.p.: 53–54 °C; IR (KBr):  $\nu_{\max}$  = 2954, 1503, 1427, 1221  $\text{cm}^{-1}$ ;  $^1\text{H}$  NMR (400.13 MHz, DMSO):  $\delta$  = 5.60 (s, 1H, N–H), 7.15 (d of d,  $J$  = 14.6 Hz,  $J$  = 7.2 Hz, 2H), 7.25 (d of d,  $J$  = 14.6 Hz,  $J$  = 7.2 Hz, 4H), 7.38 (d,  $J$  = 2.4 Hz, 4H) ppm.;  $^{13}\text{C}$  NMR (100.6 MHz, DMSO):  $\delta$  = 119.9, 121.0, 123.7, 136.3 ppm.

4-Methyl-*N*-phenylaniline (Table 4, entry 3): m.p.: 65–66 °C; IR (KBr):  $\nu_{\max}$  = 2953, 1528, 1435, 1216  $\text{cm}^{-1}$ ;  $^1\text{H}$  NMR (400.13 MHz, DMSO):  $\delta$  = 2.28 (s, 3H,  $\text{CH}_3$ ), 5.61 (s, 1H, N–H), 7.10–7.16 (m, 2H), 7.21–7.27 (m, 3H), 7.42 (d,  $J$  = 2.0 Hz, 2H), 7.56 (d,  $J$  = 2.0 Hz, 2H) ppm.;  $^{13}\text{C}$  NMR (100.6 MHz, DMSO):  $\delta$  = 122.2, 123.0, 123.7, 123.9, 127.4, 131.5, 135.3, 135.9 ppm.

*N*-(4-Chloro-2,6-dimethylphenyl)-4-nitroaniline (Table 4, entry 11): m.p.: 78–79 °C;  $^1\text{H}$  NMR (400.13 MHz, DMSO):  $\delta$  = 2.12 (s, 6H, 2 $\text{CH}_3$ ), 5.59 (s, 1H, N–H), 7.32 (d,  $J$  = 6.6 Hz, 2H), 7.42 (s, 2H), 7.50 (d,  $J$  = 6.6 Hz, 2H) ppm.;  $^{13}\text{C}$  NMR (100.6 MHz, DMSO):  $\delta$  = 20.2, 113.1, 115.7, 122.0, 127.1, 127.5, 132.0, 136.5, 137.0 ppm.; anal. calcd. for  $\text{C}_{14}\text{H}_{13}\text{ClN}_2\text{O}_2$  (276.07): C, 60.77; H, 4.74; N, 10.12%; found: C, 61.11; H, 4.77; N, 9.99%.

*N*-(2,6-Dimethoxyphenyl)-4-nitroaniline (Table 4, entry 11): m.p.: 85–87 °C;  $^1\text{H}$  NMR (400.13 MHz, DMSO):  $\delta$  = 3.87 (s, 6H, 2 $\text{OCH}_3$ ), 5.54 (s, 1H, N–H), 6.88 (s, 2H), 6.97 (s, 1H), 7.15 (d,  $J$  = 6.8 Hz, 2H), 7.34 (d,  $J$  = 6.8 Hz, 2H) ppm.;  $^{13}\text{C}$  NMR (100.6 MHz, DMSO):  $\delta$  = 50.1, 113.5, 114.4, 121.8, 124.0, 126.8, 128.8, 129.2,

130.3 ppm.; anal. calcd. for  $C_{14}H_{14}N_2O_4$  (274.10): C, 61.31; H, 5.14; N, 10.21%; found: C, 61.60; H, 5.18; N, 10.08%.

## Results and discussion

### Characterization of the catalyst

#### FT-IR spectra of the catalyst

The FT-IR spectra of AMBA-MNPs, IS-AMBA-MNPs and Cu-IS-AMBA-MNPs are displayed in Fig. 1. The peaks of  $Fe_3O_4$  appeared at 624 and 570  $cm^{-1}$ , which can be ascribed to the stretching vibrations of the Fe–O bond. The monitored peaks at 3450 and around 2923 and 2860  $cm^{-1}$  in the FT-IR spectrum of AMBA-MNPs correspond to the N–H and C–H stretching bands of the alkyl chain, respectively. The adsorption peaks at 1632, 1375 and 1086  $cm^{-1}$  are related to the asymmetric

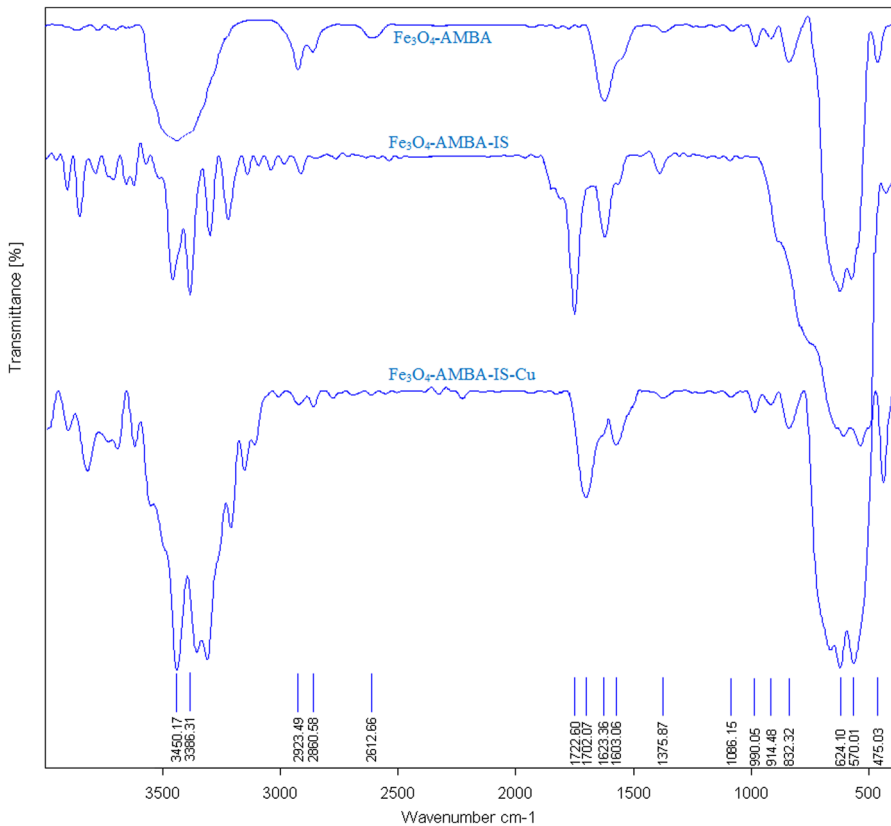


Fig. 1 FT-IR spectra for AMBA-MNPs, IS-AMBA-MNPs and Cu-IS-AMBA-MNPs

and symmetric stretching vibration of COO (carboxylate group) of the 4-(aminomethyl)benzoic acid moiety. In the FT-IR spectrum of IS-AMBA-MNPs, new bands were observed at 1623 and 1722  $\text{cm}^{-1}$  due to the C=N and C=O stretching vibration bands, respectively. These bands confirmed that isatin has been successfully reacted with the amino present in the structure of the AMBA-MNPs. The N-H stretching peak of the amide group in isatin appeared at 3386  $\text{cm}^{-1}$ . In the FT-IR spectra of Cu-IS-AMBA-MNPs (Fig. 1), the C=N and C=O stretching bands were shifted to the lower wave numbers (1600 and 1706  $\text{cm}^{-1}$ ), which revealed the successful coordination of nitrogen and oxygen to the metal center.

### XRD pattern analysis of the catalyst

Powder X-ray diffraction patterns of the IS-AMBA-MNPs and Cu-IS-AMBA-MNPs are shown in Fig. 2. The reflection planes of X-ray diffraction using a  $\text{CuK}\alpha$  irradiation was applied to characterize the demonstration of the crystal structure of the samples after the functionalization step. As shown in Fig. 2, the peaks at  $2\theta=42.87^\circ$ ,  $50.26^\circ$  and  $74.56^\circ$  assigned with the (111), (200) and (220) planes were attributed to Cu (II) [8]. Also,  $2\theta=30.2^\circ$ ,  $35.30^\circ$ ,  $43.3^\circ$ ,  $53.65^\circ$ ,  $57.3^\circ$ , and  $62.8^\circ$  peaks corresponding to the (220), (311), (400), (422), (511), and (440) planes were obtained due to the cubic spinel structure of  $\text{Fe}_3\text{O}_4$  NPs. The results are in good agreement with standard patterns of the inverse cubic spinel magnetite crystal structure (JCPDS No. 19-0629). The prepared sample has good crystallinity due to the presence of sharp peaks in the XRD pattern. The crystallite size of the catalyst was

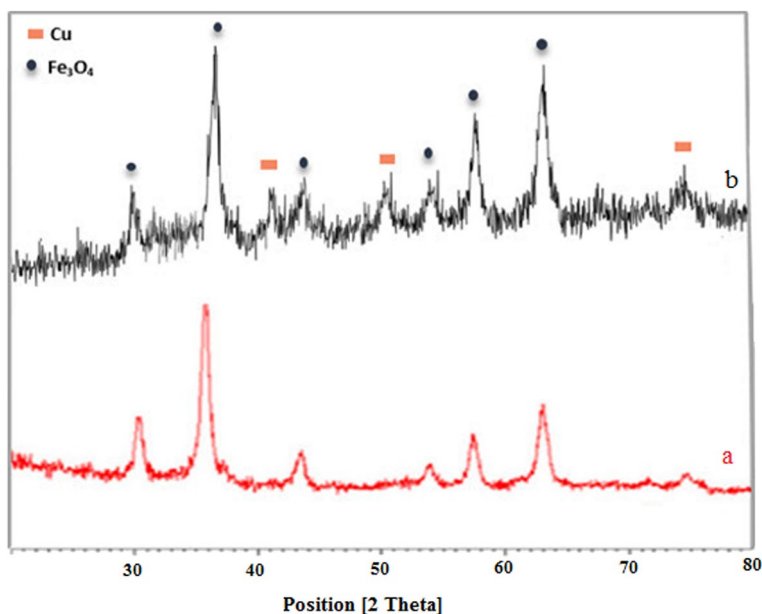


Fig. 2 XRD patterns of IS-AMBA-MNPs (a) and Cu-IS-AMBA-MNPs (b)



evaluated and was found to be 18 nm using Scherrer's formula based on the XRD peak at 30.

### TGA analysis of the catalyst

The thermal behavior of Cu-IS-AMBA-MNPs was studied by TGA under an air atmosphere with a heating rate of  $10\text{ }^{\circ}\text{C min}^{-1}$  within a temperature range of  $0\text{--}650\text{ }^{\circ}\text{C}$  (Fig. 3). The composition ratio of the catalyst can be estimated from the residual mass percentage. As shown in Fig. 3, the first weight loss stage at nearly  $100\text{ }^{\circ}\text{C}$  (0.52%) was assigned to the evaporation of adsorbed water molecules. The second weight loss at  $100\text{--}400\text{ }^{\circ}\text{C}$  (8.0%) can be ascribed to loss of  $\text{CuCl}_2$  and the isatin group. The final weight loss at  $400\text{ to }650\text{ }^{\circ}\text{C}$  (5.11%) corresponds to 4-(aminomethyl)benzoate. On the basis of these results, the good grafting of AMBA-IS-Cu on the  $\text{Fe}_3\text{O}_4$  nanoparticles is confirmed.

### SEM images of the catalyst

The SEM images of the AMBA-MNPs and Cu-IS-AMBA-MNPs are presented in Fig. 4, according to which the SEM image of the supported nanocatalyst has a spherical morphology and good dispersity. It was estimated to have individual crystallite sizes ranging 10 and 30 nm.

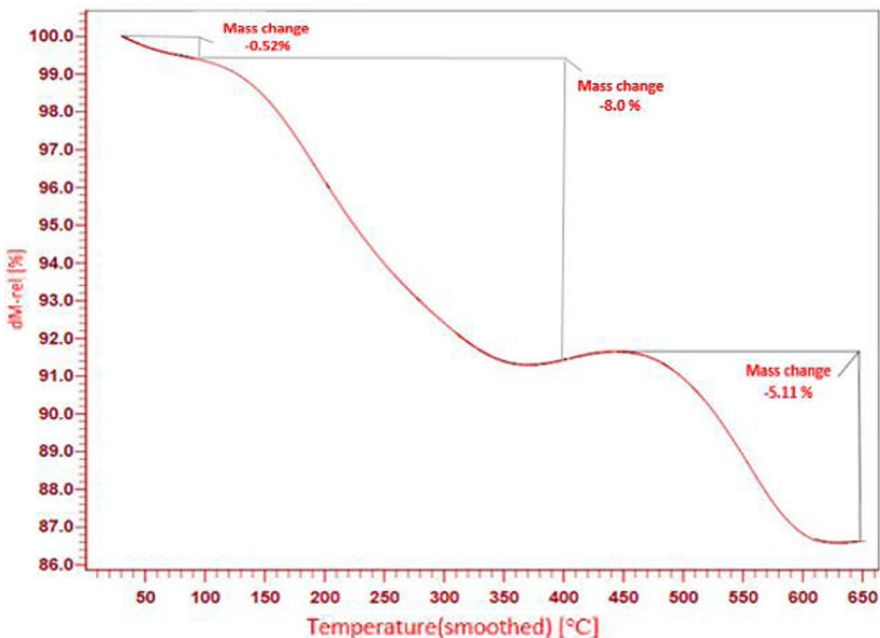
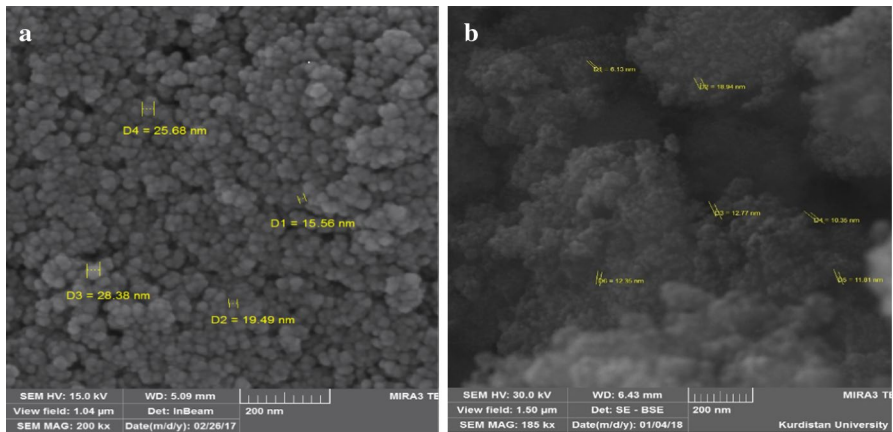


Fig. 3 TGA diagram of Cu-IS-AMBA-MNPs



**Fig. 4** SEM images of AMBA-MNPs (a) and Cu-IS-AMBA-MNPs (b)

### EDX analysis of the catalyst

The EDX analysis of Cu-IS-AMBA-MNPs is displayed in Fig. 5, from which it can be seen that Cu-IS-AMBA-MNPs is composed of the expected elements in the structure of the catalyst, namely carbon (C), oxygen (O), nitrogen (N), iron (Fe), copper (Cu) and chlorine (Cl), indicating that Cu has been properly connected to IS-AMBA-MNPs.

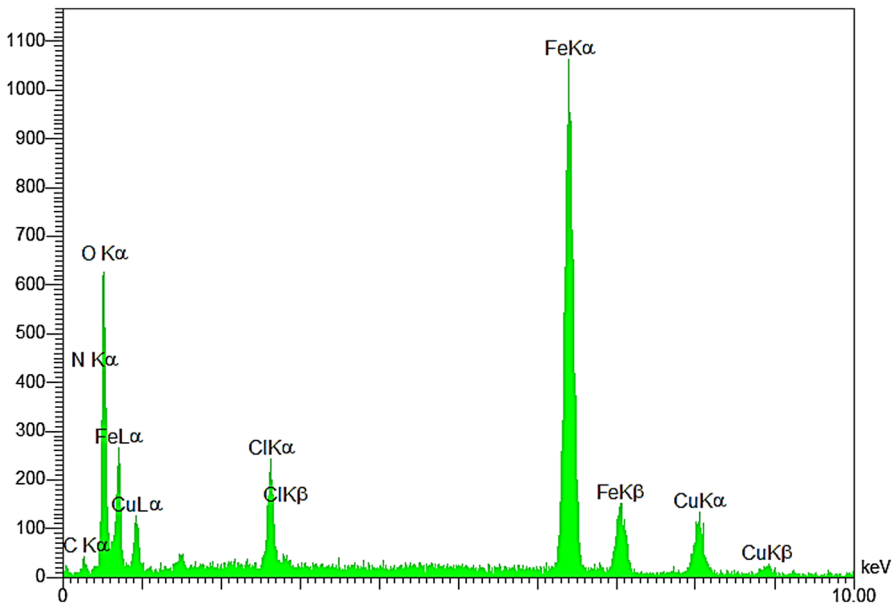


**Fig. 5** EDX spectrum of Cu-IS-AMBA-MNPs

## Magnetic properties of the catalyst

The magnetic properties of the AMBA-MNPs, IS-AMBA-MNPs, and Cu-IS-AMBA-MNPs were characterized by VSM at 300 K (Fig. 6). The magnetization curves for these nanoparticles show no hysteresis in their magnetizations. Moreover, the absence of coercivity and remanence for the three nanoparticles indicate that these nanoparticles were superparamagnetic. The saturation magnetization values for AMBA-MNPs, IS-AMBA-MNPs, and, Cu-IS-AMBA-MNPs were 69.2, 54.5 and 42.6 emu g<sup>-1</sup>, respectively. A low decrease of the saturation magnetization of Cu-IS-AMBA-MNPs occurred because of the connection of Cu on the surface of the IS-AMBA-MNPs nanoparticles. In other words, these differences are due to the various coating layers and their thicknesses on the surface of the MNPs. However, the prepared magnetite catalyst still has good magnetic properties and can be easily, quickly and completely separated from the reaction medium by a magnetic field.

## Catalytic application of the catalyst

The catalytic activity of the nanocatalyst was evaluated by using Cu-IS-AMBA-MNPs to synthesis diphenyl ether from the reaction of iodobenzene and phenol. For optimization of the conditions, the effect of solvent, temperature and the amount of the catalyst was studied in this reaction. As can be seen in Table 1, the nature of the solvent affects the efficiency of the coupling reaction (Table 1, entries 1–5). It was found that DMF was the best among the other solvents, which included CH<sub>3</sub>OH, CH<sub>3</sub>CN, H<sub>2</sub>O, and DMSO, but none were as effective as DMF. Another efficient factor in the catalytic performance of Cu-IS-AMBA-MNPs is the amount of the catalyst based on the obtained results. The reaction was performed with various amounts of the catalyst (40, 50, and 60 mg), and the best performance was obtained when

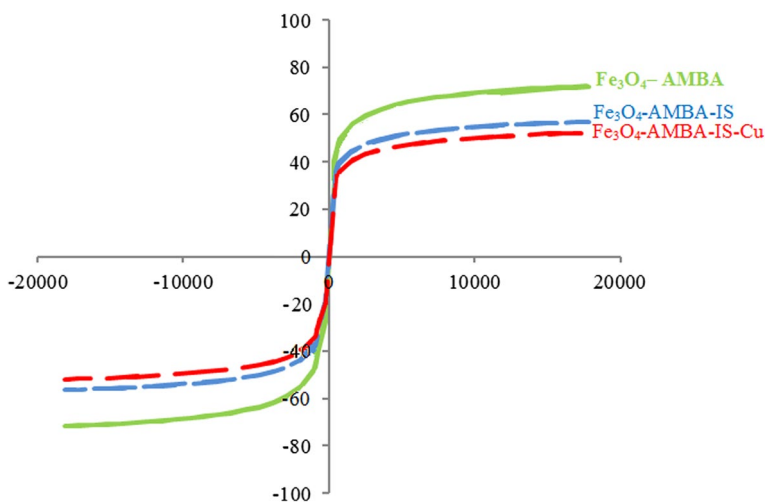


**Fig. 6** Magnetization curves of AMBA-MNPs, IS-AMBA-MNPs and Cu-IS-AMBA-MNPs

**Table 1** Optimization of the reaction conditions in the synthesis of **3a**

Entry	Catalyst	Solvent	Amount of the catalyst (mg)	Temperature (°C)	Time (h)	Yield (%) <sup>a</sup>
1	Cu-IS-AMBA-MNPs	CH <sub>3</sub> OH	40	60	4	32
2	Cu-IS-AMBA-MNPs	CH <sub>3</sub> CN	40	60	4	35
3	Cu-IS-AMBA-MNPs	H <sub>2</sub> O	40	60	4	21
4	Cu-IS-AMBA-MNPs	DMSO	40	60	4	31
5	Cu-IS-AMBA-MNPs	DMF	40	60	4	38
6	Cu-IS-AMBA-MNPs	CH <sub>3</sub> OH	40	Reflux	4	58
7	Cu-IS-AMBA-MNPs	CH <sub>3</sub> CN	40	Reflux	4	60
8	Cu-IS-AMBA-MNPs	H <sub>2</sub> O	40	Reflux	4	38
9	Cu-IS-AMBA-MNPs	DMSO	40	100	4	55
10	Cu-IS-AMBA-MNPs	DMF	40	100	4	77
11	Cu-IS-AMBA-MNPs	DMSO	40	110	4	79
12	Cu-IS-AMBA-MNPs	DMF	40	110	4	84
13	Cu-IS-AMBA-MNPs	DMF	50	110	3	98
14	Cu-IS-AMBA-MNPs	DMF	60	110	3	98
15	CuCl <sub>2</sub>	DMF	50	110	3	68
16	–	DMF	50	110	3	–

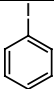
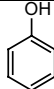
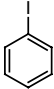
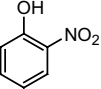
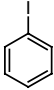
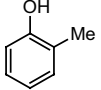
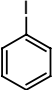
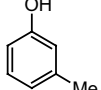
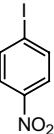
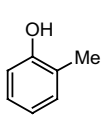
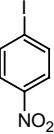
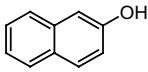
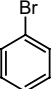
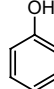
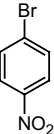
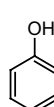
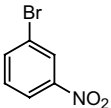
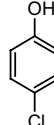
<sup>a</sup>Yields refer to isolated products

50 mg of the catalyst (0.02 mmol%) was used. Finally, the effect of temperature was investigated and the best result was obtained at 110 °C in the presence of 50 mg (0.02 mmol) of the catalyst using 5 mL of DMF. The control experiment shows that *O*-arylation did not occur in the absence of the catalyst (Table 1, entry 16).

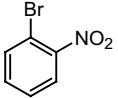
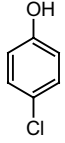
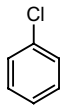
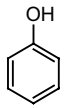
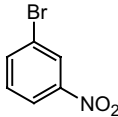
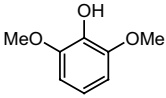
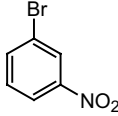
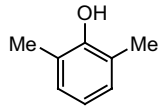
To explore the scope and limitations of this catalyst, a variety of phenols reacted with different substituted phenyl halides under the optimal reaction conditions and the results are collected in Table 2. It is shown that all of the substrates reacted well with high yields. In *O*-arylation, the presence of *ortho* substituents on the phenol ring was tolerated (Table 2, entries 12 and 13). In addition, *para* and *ortho* substituents on aryl halide were suitable for the preparation of diphenyl ethers. It is interesting to note that chlorobenzene tolerated the reaction conditions and gave the corresponding product in high yield. To investigate the role of immobilized copper supported on MNPs, a further experiment was carried out in the presence of CuCl<sub>2</sub> (Table 1, entry 15). Based on the results gained in the presence of CuCl<sub>2</sub>, the obtained yield is not comparable with the yield of the reaction in the presence of the catalyst. Thus, the immobilized magnetic NPs not only aid easy separation of the catalyst from the reaction mixture but also improve the yields of the reactions.

Encouraged by the satisfactory results in the synthesis of diaryl ethers, we decided to extend the investigation of the catalytic activity of Cu-IS-AMBA-MNPs into the synthesis of diphenylamine from phenyl boronic acid (1 mmol) and aniline (1.2 mmol). The effects of solvent, temperature, and the amount of Cu-IS-AMBA-MNPs were examined to optimize the reaction conditions (Table 3). Acetonitrile, methanol, water, DMF, and DMSO were evaluated as the solvent of which it was

**Table 2** Synthesis of diaryl ethers **3a–3k** in the presence of the catalyst<sup>a</sup>

Entry	Aryl halide	Phenols	Pro duct	Yield <sup>b</sup> (%)	TON <sup>c</sup>	Melting Point (°C)	
						Found	Reported [Ref]
1			3a	97	46	31-32	31 [43]
2			3b	99	47	48-49	47 - 49 [44]
3			3c	97	46	22-23	21.5 - 22 [44]
4			3d	96	45	21-22	20 [45]
5			3e	95	45	62-63	61.9 - 62.2 [45]
6			3f	97	46	97-98	96 - 98 [45]
7			3g	95	45	30-31	31[43]
8			3h	96	46	56-57	56 - 58 [46]
9			3i	96	46	62-63	63 - 64 [47]

**Table 2** (continued)

Entry	Aryl halide	Phenols	Pro duct	Yield <sup>b</sup> (%)	TON <sup>c</sup>	Melting Point (°C)	
						Found	Reported [Ref]
10			3j	95	45	45-46	46 [48]
11			3k	94	44	32-34	31 [43]
12			3l	90	42	35-37	-
13			3m	91	43	42-43	-

<sup>a</sup>Reaction conditions: Phenyl halide (1 mmol), phenol derivative (1 mmol), K<sub>2</sub>CO<sub>3</sub> (1.5 mmol), and the catalyst (0.05 g) in DMF (5 mL) at 110 °C

<sup>b</sup>Yields refer to the isolated products

<sup>c</sup>TON = (mmol of product/mmol of catalyst)

found that DMSO is the best (Table 3, entries 1–5). The temperature and catalyst loading were examined and the results show that increasing the reaction temperature or the catalyst loading leads to an increase in yield (Table 3, entries 6–10, 13, 14). Thus, the optimal conditions were 0.06 g (0.025 mmol) of Cu-IS-AMBA-MNPs in DMSO (4 mL) solvent at 130 °C in 2 h, and the yield of product was 97%.

The generality and applicability of this catalyst in the synthesis of diarylamines were investigated under the optimized reaction conditions. The results in Table 4 show that anilines and phenylboronic acid derivatives with both electron-withdrawing and electron-releasing groups reacted efficiently and afforded the products with excellent yields. *N*-arylation of iodobenzene afforded similar results to the bromobenzene.

The most important advantages of heterogeneous solid catalysts in organic reactions are recoverability and reusability. Thus, the recoverability and reusability of the catalyst were investigated using the selected model reaction of iodobenzene and phenol in DMF (Table 2, entry 1). The reaction mixture was cooled to room temperature when the reaction was complete. Then, the catalyst was recovered by a

**Table 3** Optimization of the reaction conditions in the synthesis of **6a**

Entry	Catalyst	Solvent	Amount of the catalyst (mg)	Temperature (°C)	Time (h)	Yield (%) <sup>a</sup>
1	Cu-IS-AMBA-MNPs	CH <sub>3</sub> OH	40	60	4	32
2	Cu-IS-AMBA-MNPs	CH <sub>3</sub> CN	40	60	4	30
3	Cu-IS-AMBA-MNPs	H <sub>2</sub> O	40	60	4	22
4	Cu-IS-AMBA-MNPs	DMF	40	60	4	33
5	Cu-IS-AMBA-MNPs	DMSO	40	60	4	42
6	Cu-IS-AMBA-MNPs	CH <sub>3</sub> OH	40	Reflux	4	45
7	Cu-IS-AMBA-MNPs	CH <sub>3</sub> CN	40	Reflux	4	48
8	Cu-IS-AMBA-MNPs	H <sub>2</sub> O	40	Reflux	4	20
9	Cu-IS-AMBA-MNPs	DMF	40	100	4	65
10	Cu-IS-AMBA-MNPs	DMSO	40	100	4	72
11	Cu-IS-AMBA-MNPs	DMF	40	130	2	78
12	Cu-IS-AMBA-MNPs	DMSO	40	130	2	80
13	Cu-IS-AMBA-MNPs	DMSO	50	130	2	95
14	Cu-IS-AMBA-MNPs	DMSO	60	130	2	97
15	CuCl <sub>2</sub>	DMSO	60	130	2	62

<sup>a</sup>Yields refer to isolated products

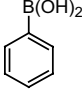
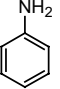
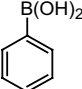
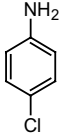
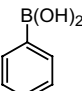
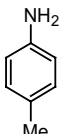
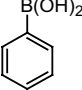
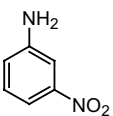
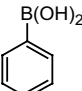
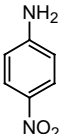
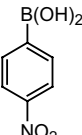
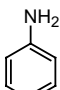
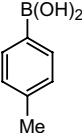
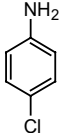
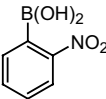
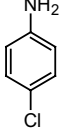
magnetic field, washed with water and ethanol, and dried for the next run. According to the obtained results, the catalyst has good activity, reusability, and stability in the reaction media and could be reused five times with no loss of activity (Fig. 7). The reaction in the absence of the catalyst under the same conditions afforded no product. The concentration of Cu in the catalyst was 2.7 wt% (0.42 mmol g<sup>-1</sup>) which was determined using ICP-AES.

The capability and efficiency of the catalyst compared with the catalysts reported in the literature for the synthesis of diphenyl ether and diphenylamine derivatives were studied. Thus, the reactions of phenyl iodide with phenol and boronic acid with aniline were examined as representative examples and conducted in the presence of different catalysts. The results indicate that these methods are comparable to some previously reported methods in terms of reaction times and yields (Tables 5, 6).

## Conclusion

A new and efficient copper–isatin complex supported on 4-(aminomethyl) benzoic acid-functionalized Fe<sub>3</sub>O<sub>4</sub> nanoparticles has been developed as a highly active and recoverable heterogeneous and stable catalyst for the preparation of diaryl ethers and diarylamines. These compounds were synthesized via the Ullmann coupling reaction between aryl halides with phenols and boronic acid with arylamines. The catalyst could be reused for several sequential cycles with no marked loss of its activity.

**Table 4** Synthesis of diarylamines **6a-6 k** in the presence of the catalyst<sup>a</sup>

Entry	Boronic acid	Aniline	Product	Yield <sup>b</sup> (%)	TON	Melting Point (°C)	
						Found	Reported [Ref]
1			6a	95	38	53-54	52 - 54 [49]
2			6b	97	39	64-66	65 - 66 [50]
3			6c	95	38	91-92	90 [51]
4			6d	96	38.5	84-85	85 - 87 [49]
5			6e	98	39.2	137	135 - 136 [51]
6			6f	95	38	136-137	135 - 136 [51]
7			6g	96	38.4	80-82	81 - 83 [52]
8			6h	95	38	136-137	135 - 137 [53]

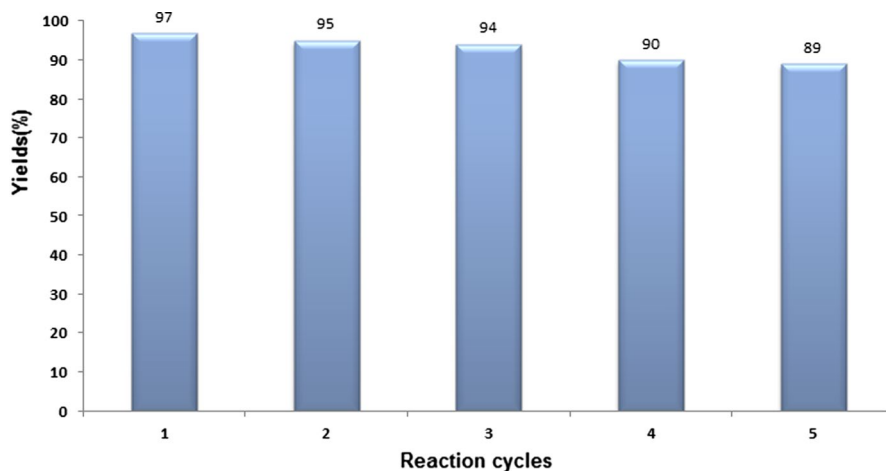


**Table 4** (continued)

Entry	Boronic acid	Aniline	Product	Yield <sup>b</sup> (%)	TON	Melting Point (°C)	
						Found	Reported [Ref]
9			6i	97	39	91-92	90 [51]
10			6j	98	39.2	72-74	73 - 75 [49]
11			6k	94	37	78-79	-
12			6l	92	36	85-87	-

<sup>a</sup>Reaction conditions: Aniline (1.2 mmol), boronic acid (1 mmol), KF (2 mmol), and the catalyst (0.06 g) in DMSO (4 mL) at 130 °C

<sup>b</sup>Yields refer to the isolated products

**Fig. 7** Reusability of the catalyst

**Table 5** Comparison of the results of this catalyst with other catalysts reported in the synthesis of diphenyl ether

Entry	Catalyst	Conditions	Time	Yield (%) <sup>a</sup> [References]
1	Cu <sub>2</sub> O nanocubes (0.1 mol%), Cs <sub>2</sub> CO <sub>3</sub> (2 eq)	THF (10 ML), 150 °C	3 h	90 [13]
2	Potassium Fluoride Supported on Natural Nanoporous Zeolite (0.62 g), KF (0.3 mol %)	DMSO (4–6 ML), 115 °C	2 h	95 [53]
3	Fe <sub>3</sub> O <sub>4</sub> @mesoporouspolyaniline (25 mg), K <sub>2</sub> CO <sub>3</sub> (1.5 mmol)	DMF (2 ML), 135 °C	12 h	95 [53, 54]
4	Copper(II) trans bis (glycinato) (2 mol %), KOH (2 mmol)	DMSO (2 ML), 80 °C	8 h	98 [55]
5	CuI (1 mol %), Fe(acac) <sub>3</sub> (2 mol %)	DMF (0.8 ML), 135 °C	12 h	95 [56]
6	MNPs (0.05 g), K <sub>2</sub> CO <sub>3</sub> (1.5 mmol)	DMF (5 ML), 110 °C	24 h	No reaction
7	AMBA-MNPs (0.05), K <sub>2</sub> CO <sub>3</sub> (1.5 mmol)	DMF (5 ML), 110 °C	24 h	No reaction
8	IS-AMBA-MNPs (0.05), K <sub>2</sub> CO <sub>3</sub> (1.5 mmol)	DMF (5 ML), 110 °C	24 h	No reaction
9	Cu-IS-AMBA-MNPs (0.05 g, 0.02 mmol), K <sub>2</sub> CO <sub>3</sub> (1.5 mmol)	DMF (5 ML), 110 °C	3 h	97 (Present work)

<sup>a</sup>Isolated yield

**Table 6** Comparison of the results of this catalyst with other catalysts reported in the synthesis of diphenylamine

Entry	Catalyst	Conditions	Time	Yield (%) <sup>a</sup> [References]
1	Cu <sub>2</sub> -β-CD (0.01 mmol), K <sub>2</sub> CO <sub>3</sub> (3 equiv.)	DMF (1 ML), 90 °C	48 h	90 [57]
2	Cu(OAc) <sub>2</sub> (5-20 mol %), myristic acid (10-40 mol %)	Toluene (2 ML), r.t	24 h	92 [58]
3	CuFAP (100 mg)	Methanol (4 ML), r.t	3 h	90 [59]
4	MNPs(0.06 g), KF (2 mmol)	DMSO (4 ML), 130 °C	24 h	No reaction
5	AMBA-MNPs (0.06 g), KF(2 mmol)	DMSO (4 ML), 130 °C	24 h	No reaction
6	IS-AMBA-MNPs (0.06 g), KF(2 mmol)	DMSO (4 ML), 130 °C	24 h	No reaction
7	Cu-IS-AMBA-MNPs ((0.06 g, 0.025 mmol), KF (2 mmol)	DMSO (4 ML), 130 °C	2 h	96 (Present work)

<sup>a</sup>Isolated yield

**Acknowledgement** We thank the Research Council of Razi University for generous financial support of this work.

## References

1. J.S. Sawyer, *Tetrahedron* **56**, 5045 (2000)
2. X. Zhang, F. Liu, Z. Wei, Z.O. Wang, *Lett. Org. Chem.* **10**, 31 (2013)
3. H.J. Cristau, P.P. Cellier, S. Hamada, J.F. Spindler, M. Taillefer, *Org. Lett.* **6**, 913 (2004)
4. K.C. Nicolaou, C.N.C. Boddy, S. Brase, N. Winssinger, *Angew. Chem. Int. Ed.* **38**, 2096 (1999)
5. K.C. Nicolaou, S. Natarajan, H. Li, N.F. Jain, R. Huges, M.E. Solomon, J.M. Ramanujulu, C.N.C. Boddy, M. Takayanagi, *Angew. Chem. Int. Ed.* **37**, 2708 (1998)
6. Q. Zhang, D.P. Wang, X.Y. Wang, K. Ding, *J. Org. Chem.* **74**, 7187 (2009)
7. F. Ullmann, *Chem. Ber. Dtsch. Chem. Ges.* **37**, 853 (1904)
8. A. Shaabani, S.E. Afshari, R. Hooshmand, A.T. Tabatabaei, F. Hajishaabanha, *RSC Adv.* **6**, 18113 (2016)
9. J. Lindley, *Tetrahedron* **40**, 1433 (1984)
10. J.C. Henrim, P.C. Pascal, H. Samy, F.S. Jean, *Org. Lett.* **6**, 913 (2004)
11. Y. Zhang, G. Ni, C. Li, S. Xu, Z. Zhang, X. Xie, *Tetrahedron* **71**, 4927 (2015)
12. S. Handa, Y. Wang, F. Gallou, B.H. Lipshutz, *Science* **349**, 1087 (2015)
13. J.Y. Kim, J.C. Park, A. Kim, A.Y. Kim, H.J. Lee, H. Song, K.H. Park, *Eur. J. Inorg. Chem.* **28**, 4219 (2009)
14. K. Huang, Y. Chen, J.H. Chan, L.R. Mike, D.L. Robert, *Synlett* **10**, 1419 (2011)
15. V.R. Choudhary, D.K. Dumbre, P.N. Yadav, S.K. Bhargava, *Catal. Commun.* **29**, 132 (2011)
16. S.A.R. Mulla, S.M. Inamdar, M.Y. Pathan, S.S. Chavan, *Tetrahedron Lett.* **53**, 1826 (2012)
17. F. Zhou, J. Guo, J. Liu, K. Ding, S. Yu, Q. Cai, *J. Am. Chem. Soc.* **134**, 14326 (2012)
18. S.G. Babu, R. Karvembu, *Tetrahedron Lett.* **54**, 1677 (2013)
19. R.K. Gujadhur, C.G. Bates, D. Venkataraman, *Org. Lett.* **3**, 4315 (2001)
20. F.Y. Kwong, A. Klapars, S.L. Buchwald, *Org. Lett.* **4**, 581 (2002)
21. H.J. Cristau, P.P. Cellier, J.F. Spindler, M. Taillefer, *Org. Lett.* **6**, 913 (2004)
22. S. Zhang, D. Zhang, L.S. Liebeskind, *J. Org. Chem.* **62**, 2312 (1997)
23. A.A. Kelkar, N.M. Patil, R.V. Chaudhari, *Tetrahedron Lett.* **43**, 7143 (2002)
24. A.S. Gajare, K. Toyota, M. Yoshifuji, F. Yoshifuji, *Chem. Commun.* **17**, 1994 (2004)
25. E. Buck, Z.J. Song, D. Tschäen, P.G. Dormer, R.P. Volante, P.J. Reider, *Org. Lett.* **4**, 1623 (2002)
26. C. Palomo, M. Oiarbide, R. Lopez, E. Gomez-Bengoa, *Chem. Commun.* **19**, 2091 (1998)
27. D. Ma, Q. Cai, *Org. Lett.* **5**, 3799 (2003)
28. N.K. Ojha, G.V. Zyryanov, A. Majee, V.N. Charushin, O.N. Chupakhin, S. Santra, *Coord. Chem. Rev.* **353**, 1 (2017)
29. J.S. Zheng, X.S. Zhang, P. Li, J. Zhu, X.G. Zhou, W.K. Yuan, *Electrochem. Commun.* **9**, 895 (2007)
30. W. Wu, Q. He, C. Jiang, *Nanoscale Res. Lett.* **3**, 397 (2008)
31. A. Wang, X. Liu, Z. Su, H. Jing, *Catal. Sci. Tech.* **4**, 71 (2014)
32. S. Fan, W. Dong, X. Huang, H. Gao, J. Wang, Z. Jin, J. Tang, G. Wang, *ACS Catal.* **7**, 243 (2016)
33. K. Mishra, T.N. Poudel, N. Basavegowda, Y.R. Lee, *J. Catal.* **344**, 273 (2016)
34. H.N. Dadhania, K.R. Dipak, N.D. Abhishek, *Catal. Sci. Tech.* **5**, 4806 (2015)
35. X. An, D. Cheng, L. Dai, B. Wang, H.J. Ocampo, J. Nasrallah, X. Jia, J. Zou, Y. Long, Y. Ni, *Appl. Catal. B* **206**, 53 (2017)
36. M.A. Zolfigol, V. Khakyzadeh, A.R. Moosavi-Zare, A. Rostami, A. Zare, N. Iranpoor, R. Luque, *Green Chem.* **15**, 2132 (2013)
37. M. M. Khodaei, A. Alizadeh, M. Haghypour, *Res. Chem. Inter.* (2017). <https://doi.org/10.1007/s11164-017-3008-2>
38. K. He, Y. Ma, B. Yang, C. Liang, X. Chen, C. Cai, *Mol. Biomol. Spectrosc.* **173**, 82 (2017)
39. S. Liu, H. Wang, L. Chai, M. Li, *J. Coll. Inter. Sci.* **478**, 288 (2016)
40. R. Mirzajani, S. Ahmadi, *J. Ind. Eng. Chem.* **23**, 171 (2015)
41. M.A. Rahman, U. Culsum, A. Kumar, H. Gao, N. Hu, *Int. J. Biol. Macromolec.* **87**, 488 (2016)
42. D. Yang, J. Hu, S. Fu, *J. Phys. Chem. C* **113**, 7646 (2009)
43. R. Singh, B.K. Allam, D.S. Raghuvanshi, K.N. Singh, *Tetrahedron* **69**, 1038 (2013)

44. J.C. Vantourout, R.P. Law, A. Isidro-Llobet, S.J. Atkinson, A.J. Watson, *J. Org. Chem.* **81**, 3942 (2016)
45. A. Ghorbani-Choghamarani, Z. Taherinia, Z. New J. Chem. **41**, 9414 (2017)
46. L. Cai, X. Qian, W. Song, T. Liu, X. Tao, W. Li, X. Xie, *Tetrahedron* **70**, 4754 (2014)
47. J. Liu, D. Yang, X. Yang, M. Nie, G. Wu, Z. Wang, P. Gong, *Bio. Med. Chem.* **25**, 4475 (2017)
48. K. Kulangiappar, M. Anbukulandainathan, T. Raju, *Synth. Commun.* **1**, 2494 (2014)
49. S. Yamada, M. Ishikawa, C. Kaneko, *Chem. Pharm. Bull.* **23**, 2818 (1975)
50. A. Kumar, B.S. Bhakuni, C.D. Prasad, S. Kumar, S. Kumar, *Tetrahedron* **69**, 5383 (2013)
51. H. Xu, Y. Chen, *Synth. Commun.* **37**, 2411 (2007)
52. F. Damkaci, C. Sigindere, T. Sobiech, E. Vik, J. Malone, *Tetrahedron Lett.* **58**, 3559 (2017)
53. M. Khalilzadeh, A. Hosseini, A. Pilevar, *Eur. J. Org. Chem.* **8**, 1587 (2011)
54. R. Arundhathi, D. Damodara, P.R. Likhari, M.L. Kantam, P. Saravanan, T. Magdaleno, S.H. Kwon, *Adv. Syn. Catal.* **353**, 1591 (2011)
55. S. Verma, N. Kumar, S.L. Jain, *Tetrahedron Lett.* **53**, 4665 (2012)
56. X. Liu, S. Zhang, *Synlett* **2**, 268 (2011)
57. B. Kaboudin, Y. Abedi, T. Yokomatsu, *Eur. J. Org. Chem.* **33**, 6656 (2011)
58. J.C. Antilla, S.L. Buchwald, *Org. Lett.* **3**, 2077 (2001)
59. M.L. Kantam, G.T. Venkanna, C. Sridhar, B. Sreedhar, B.M. Choudary, *J. Org. Chem.* **71**, 9522 (2006)

**Publisher's Note** Springer Nature remains neutral with regard to jurisdictional claims in published maps and institutional affiliations.